

DOI 10.24425/aee.2023.146040

# Photovoltaic power prediction based on improved grey wolf algorithm optimized back propagation

PING HE ✉, JIE DONG , XIAOPENG WU , LEI YUN , HUA YANG 

Zhengzhou University of Light Industry, College of Electrical and Information Engineering  
China

e-mail: ✉ [hplkz@126.com](mailto:hplkz@126.com), [\[1365314213/642183255/871454827\]@qq.com](mailto:[1365314213/642183255/871454827]@qq.com), [xpwu@zzuli.edu.cn](mailto:xpwu@zzuli.edu.cn)

(Received: 05.12.2022, revised: 29.03.2022)

**Abstract:** At present, the back-propagation (BP) network algorithm widely used in the short-term output prediction of photovoltaic power stations has the disadvantage of ignoring meteorological factors and weather conditions in the input. The existing traditional BP prediction model lacks a variety of numerical optimization algorithms, such that the prediction error is large. The back-propagation (BP) neural network is easy to fall into local optimization thus reducing the prediction accuracy in photovoltaic power prediction. In order to solve this problem, an improved grey wolf optimization (GWO) algorithm is proposed to optimize the photovoltaic power prediction model of the BP neural network. So, an improved grey wolf optimization algorithm optimized BP neural network for a photovoltaic (PV) power prediction model is proposed. Dynamic weight strategy, tent mapping and particle swarm optimization (PSO) are introduced in the standard grey wolf optimization (GWO) to construct the PSO–GWO model. The relative error of the PSO–GWO–BP model predicted data is less than that of the BP model predicted data. The average relative error of PSO–GWO–BP and GWO–BP models is smaller, the average relative error of PSO–GWO–BP model is the smallest, and the prediction stability of the PSO–GWO–BP model is the best. The model stability and prediction accuracy of PSO–GWO–BP are better than those of GWO–BP and BP.

**Key words:** BP neural network, photovoltaic power generation, PSO–GWO model, PSO–GWO–BP prediction model, standard grey wolf algorithm



© 2023. The Author(s). This is an open-access article distributed under the terms of the Creative Commons Attribution-NonCommercial-NoDerivatives License (CC BY-NC-ND 4.0, <https://creativecommons.org/licenses/by-nc-nd/4.0/>), which permits use, distribution, and reproduction in any medium, provided that the Article is properly cited, the use is non-commercial, and no modifications or adaptations are made.

## 1. Introduction

Under the background of “carbon peaking and carbon neutrality”, clean energy has been developed rapidly. As a new type of renewable energy, solar energy has many advantages, such as convenient collection, wide distribution, clean without pollution [1–3]. Therefore, scholars have carried out a lot of research on photovoltaic (PV) power generation technology at home and abroad. Although PV generation has unique advantages that other renewable energy sources do not have, the disadvantages of photovoltaic power generation are also obvious. In the PV power generation systems, PV power generation is easily affected by solar radiation intensity and meteorological factors, resulting in large output power fluctuations and significant intermittency. In addition, the security, stability and reliability of the grid will face great challenge after the grid-connected of PV power generation [4–6]. So, it also needs to connect to other energy sources for adjustment. Therefore, the power of photovoltaic power generation system needs to be predicted. If the PV output can be accurately predicted, it will reduce the net cost of generation and the impacts on the grid security.

Traditional power prediction methods include time series methods [7] and regression analysis [8]. The disadvantage of the time series method is that it requires the high processing of data, while the regression analysis method has a disadvantage of difficult to establish a regression equation and low prediction accuracy. The artificial intelligence algorithm has the powerful adaptability and self-learning capability, and does not require explicit mathematical expressions. As a mature artificial intelligence algorithm, the neural network has been widely used in power load forecasting. The artificial neural network (ANN) has been considered an effective method to predict the output power of the PV power system. Up to now, the BP neural network [9, 10] has been one of the widely used artificial neural network models. In [11], an ensemble of optimized and diversified artificial neural networks (ANNs) for 24h-ahead predicting solar PV power production and, at the same time, quantifying the associated uncertainty that affects power production predictions is proposed. In [12], a BP neural network-based short-term power output prediction model of PV power generation was proposed, and it analyzed the main factors affecting the output of PV power generation. The regression analysis method has a disadvantage of difficult to establish a regression equation and low prediction accuracy. In [13], the traditional BP algorithm was improved to avoid local minima and speed convergence by combined increasing momentum with variable learning rate. The back-propagation (BP) network algorithm widely used in the short-term output prediction of photovoltaic power stations has the disadvantage of ignoring meteorological factors and weather conditions in the input. In [14], the PSO-BP algorithm was presented to accurately predict the PV power generation, solved the disadvantages of BP neural networks and improved algorithm accuracy and convergence time. In [15], the GWO-BP algorithm was proposed to improve global search capabilities and avoided falling into local minima.

Based on the above discussions, in this paper, the improved grey wolf algorithm with an optimal BP neural network model is proposed to predict PV power generation. It does not need strict data requirements like traditional prediction methods and includes the advantages of strong adaptability of neural networks. The algorithm combines the advantages of the PSO algorithm and GWO algorithm, it can search quickly and is not easy to fall into local optimum. In this paper, the stability and rapidity of the improved grey wolf algorithm is verified by testing the ant lion optimizer (ALO), the dragonfly algorithm (DA), the salp swarm algorithm (SSA), the mutation ant

lion optimization (MALO), the grey wolf optimization (GWO) algorithm) and the particle swarm optimization-grey wolf optimization (PSO-GWO) algorithm. Finally, the accuracy and applicability of the prediction model is verified by testing PSO-GWO-BP, GWO-BP and BP models.

## 2. Data acquisition

The data of this paper mainly come from “new energy photovoltaic power generation”, and mainly collect 5 indicators from the measured data. Among them, the photovoltaic power is the dependent variable of the prediction model, and the other five datum data are the independent variables of the prediction model. These five indicators are total radiation ( $\text{W}/\text{m}^2$ ), component temperature ( $^{\circ}\text{C}$ ), ambient temperature ( $^{\circ}\text{C}$ ), air pressure (Pa) and relative humidity (%).

## 3. Research on standard algorithm

### 3.1. Particle swarm optimization

Kennedy and Eberhart proposed a continuous or discrete space optimization algorithm based on population search in 1995. The algorithm was called the particle swarm optimization algorithm [16, 17]. The particle swarm optimization algorithm is widely used in optimization problems. Particle swarm optimization is an algorithm inspired by the predation behavior of flocks of birds or fish in nature. Each particle updates its position in the decision space at an adaptive rate to get the particles close to the required space. The optimal position of each particle and the position of the optimal particle in the particle swarm together guide the location of the search position of the particle swarm. The update of the velocity and the position of the  $i$ -th particle in the  $j$ -dimensional decision space adopts the following expression:

$$v_{i,j}^{t+1} = \omega v_{i,j}^{t+1} + c_1 r_1 (p_{\text{best}_{i,j}}^t - x_{i,j}^t) + c_2 r_2 (g_{\text{best}_j}^t - x_{i,j}^t), \quad (1)$$

$$x_{i,j}^{t+1} = x_{i,j}^t + v_{i,j}^{t+1}, \quad (2)$$

where:  $v_{i,j}^{t+1}$  is the velocity of the  $j$ -th dimension of the  $i$ -th particle at  $t$  iterations,  $x_{i,j}^{t+1}$  is the position of the  $j$ -th dimension of the  $i$ -th particle at  $t$  iterations.  $p_{\text{best}}$  is the best position in the history of individual particles,  $g_{\text{best}}$  is the global, optimal position of the particle swarm.  $c_1$ ,  $c_2$  are the learning factors,  $r_1$ ,  $r_2$  are the random numbers from 0 to 1.

The social structure of the grey wolf, which has a very strict hierarchy, has four levels of the wolf. These four types of wolves are  $\alpha$ ,  $\beta$ ,  $\delta$ ,  $\phi$ .  $\alpha$  is the wolf king of the wolf pack and makes decisions on all major issues of the whole wolf pack;  $\beta$  is the second layer of the wolf pack and mainly helps the wolf king to make decisions and order other wolves; the third layer is  $\delta$ , which is mainly responsible for sentry, reconnaissance and so on.  $\phi$  is the lowest layer in the wolf group, which follows the orders of the former third-order grey wolf in actions. These four groups of grey wolves need to cooperate with each other for hunting. The steps of grey wolf hunting are mainly the following three steps:

- 1) tracking, chasing, and approaching prey,

- 2) pursuing, encircling, and constantly harassing the prey until the prey stops moving in the process of predation,
- 3) attacking the prey.

According to the mathematical model of grey wolf hunting, the following equation can be obtained:

$$D(t) = |C \cdot p(t) - X(t)|, \quad (3)$$

$$X(t+1) = p(t) - A(t) \times D(t), \quad (4)$$

where:  $t$  is the number of iterations,  $p(t)$  is the location of the prey,  $X(t)$  is the location of the grey wolf.  $D(t)$  is the distance between the current grey wolf position and the prey position.  $A(t)$ ,  $C$  are the coefficient vectors.  $A(t)$ ,  $C$  are calculated as follows:

$$C = 2r_1, \quad (5)$$

$$A(t) = 2a(t) \times r_2 - a(t), \quad (6)$$

where:  $r_1, r_2$  are the random numbers from 0 to 1,  $a(t)$  is the convergence factor.  $\max$  is the maximum number of iterations.

$$a(t) = 2 - 2 \frac{t}{\max}. \quad (7)$$

The location of the wolf pack is determined by the three wolves  $\alpha, \beta, \delta$ . Therefore, the position of the prey can be determined by using the position of these three wolves. The mathematical expressions for the direct distance between three kinds of wolves and their prey are as follows:

$$\begin{cases} D_\alpha = |C_1 \cdot X_\alpha(t) - X(t)| \\ D_\beta = |C_1 \cdot X_\beta(t) - X(t)| \\ D_\delta = |C_1 \cdot X_\delta(t) - X(t)| \\ X_1 = X_\alpha - A_1 \cdot D_\alpha \\ X_2 = X_\beta - A_2 \cdot D_\beta \\ X_3 = X_\delta - A_3 \cdot D_\delta \end{cases}, \quad (8)$$

$$X_\phi(t+1) = \frac{X_1 + X_2 + X_3}{3}, \quad (9)$$

where  $X_\alpha, X_\beta, X_\delta$  are the optimal individuals of the three wolf packs under the current number of iterations.  $X_1, X_2, X_3$  are the current positions of the three wolves in the wolf pack.  $X_\phi(t+1)$  is the position of the bottom wolf in the wolf pack.

### 3.2. Back propagation neural network

The back-propagation neural network continuously updates the weight and threshold in a cycle until it reaches the minimum value of the initial calculation error or the total training times. The update process is shown in Fig. 1. The process is as follows:

#### 1. Parameter initialization

Firstly, the number of nodes in the input layer, hidden layer and output layer of the BP neural network is set as  $m, q$  and  $l$ , and the weights and thresholds between each neuron layer are set.

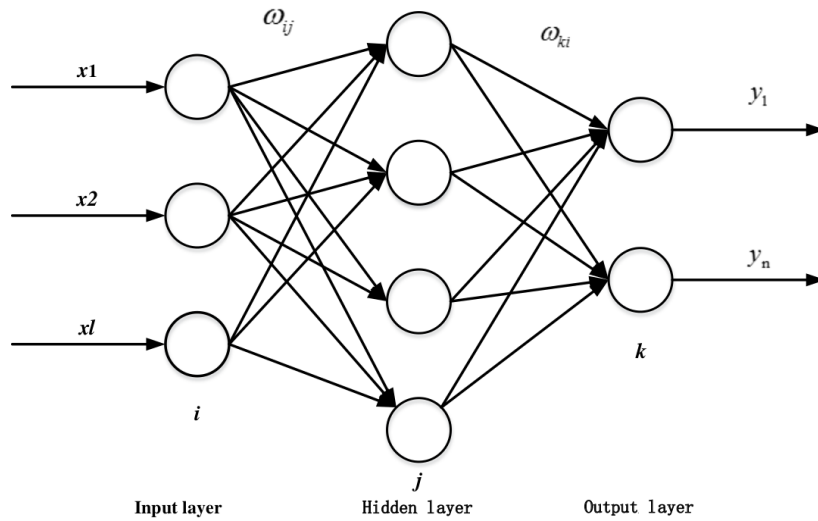


Fig. 1. Topology of BP neural network

2. Forward propagation algorithm

The output of the hidden layer of the BP neural network is shown in Eq. (10).

$$H_i = f \left( \sum_{j=1}^m \omega_{ij} - a_i \right), \quad i = 1, 2, \dots, q, \tag{10}$$

where:  $H$  is the hidden layer output,  $i$  is the input layer,  $j$  is the hidden layer,  $\omega_{ij}$  is the connection weight between the input layer and hidden layer,  $a$  is the hidden layer threshold.  $f$  is the hidden layer excitation function.

The output of the output layer is shown in Eq. (11).

$$O_k = \sum_{i=1}^q H_i \omega_{ki} - b_k, \quad k = 1, 2, \dots, L, \tag{11}$$

where:  $O$  is the output layer output,  $b$  is the output layer threshold,  $\omega_{ki}$  is the connection weight between the hidden layer and output layer.

3. The error equation, (12), for the output  $O$  and the expectation  $y'_k$  is as follows:

$$e_k = y'_k - O_k, \quad k = 1, 2, \dots, L, \tag{12}$$

where  $e_k$  is the  $k$ -th node of the error between output and expectation.

4. The update of weights and thresholds is shown in Eqs. (13) to (16).

$$\omega_{ij} = \omega_{ij} + \eta H_i (1 - H_i) x_j \sum_{k=1}^L \omega_{ki} e_k, \quad j = 1, 2, \dots, M, \tag{13}$$

$$\omega_{ki} = \omega_{ki} + \eta H_i e_k, \quad i = 1, 2, \dots, q, \quad k = 1, 2, \dots, L, \tag{14}$$

$$a_i = a_i + \eta H_i (1 - H_i) x_j \sum_{k=1}^L \omega_{ki} e_k, \quad j = 1, 2, \dots, M, \quad (15)$$

$$b_k = b_k + \eta e_k, \quad k = 1, 2, \dots, L, \quad (16)$$

where  $\eta$  is the learning efficiency.

5. Returning to step 2, if the output error is less than the set error, the calculation will end. Otherwise, the above process is repeated until the error of the BP neural network output is less than the initial set error, and the calculation is terminated.

### 3.3. Different-methodology section

The core idea of an ALO algorithm is to simulate the hunting mechanism of the ant lion hunting ants to achieve global optimization. Before hunting, the ant lion will use its huge jaw to dig a funnel-shaped trap in the sandy soil, and hide at the bottom of the trap to wait for the prey to come. Once the randomly wandering ant falls into the trap, the ant lion will quickly prey on it, and then repair the trap to wait for the next hunt. The ALO algorithm optimizes the problem through the interaction between ants and ant lions through numerical simulation: the random walk of ants is introduced to realize global search, and roulette strategy and elite strategy are used to ensure the diversity of the population and the optimization performance of the algorithm. The ant lion is equivalent to the solution of an optimization problem. It can update and save the approximate optimal solution by hunting ants being very fit.

The thaliacea is a marine invertebrate, whose body is barrel-shaped and almost completely transparent. It feeds on phytoplankton in the water and completes its movement in the water by inhaling and ejecting seawater. In the deep sea, the salps moves and forages in a chain-like group behavior, which attracts researchers' interest. The chain-like group behavior of the thallus scabbard usually forms a "chain" of individuals, which moves in turn. In the bottle scabbard chain, it is divided into leaders and followers. The leaders move towards the food and guide the movement of the following followers. The movement of the followers is only affected by the previous bottle scabbard according to the strict "hierarchy" system. Such a movement mode makes the bottle scabbard chain highly capable of global exploration and local development.

The differential evolution algorithm is a kind of adaptive global optimization algorithm based on population. It guides the optimization search by imitating the heuristic swarm intelligence generated by the cooperation and competition among individuals in the biological population. This algorithm is a kind of evolutionary algorithm, which has the advantages of simple structure, easy implementation, fast convergence and good robustness. The algorithm was first proposed by Price and Storn in 1995 and is mainly used to solve real number optimization problems. The most important operator in the differential evolution algorithm is the differential mutation operator, which differentiates and scales two individual vectors in the same group, and adds them to the third individual vector in the group to form a mutation individual vector. Then the mutation individual vector and the parent individual vector are hybridized to form the trial individual vector. Finally, try to compare the fitness value of the individual vector and the parent vector, and the better one is saved in the next generation group.

## 4. Improve grey wolf algorithm to optimize back propagation neural network

### 4.1. Improved grey wolf optimization algorithm

#### 4.1.1. Particle swarm algorithm optimization grey wolf algorithm

Although the particle swarm optimization algorithm can search quickly, it is easy to cause local optimization. The GWO algorithm can reduce the risk of falling into local optimization, but the running time of the GWO algorithm will be extended. Therefore, in order to improve the search ability of the particle swarm optimization algorithm, the particle swarm optimization grey wolf optimization (PSO–GWO) algorithm is proposed. This algorithm combines the advantages of the PSO algorithm and the GWO algorithm. To add the advantage of the powerful global search capability of the grey wolf algorithm [21, 22], the update formula of the particle swarm optimization algorithm is changed to Formula (17). It is also an update strategy of adding the grey wolf algorithm to the update formula of the particle swarm optimization algorithm.

$$v_{i,j}^{t+1} = \omega (X_{i,j}^t - x_{i,j}^t) + c_1 r_1 (p_{best_{i,j}}^t - x_{i,j}^t) + c_2 r_2 (g_{best}^t - x_{i,j}^t). \quad (17)$$

From Eq. (17), it can be seen that in the position update process of the particle swarm optimization algorithm, the original individual experience and optimal particle guidance of the particle swarm algorithm are retained, and the grey wolf algorithm update strategy  $X_\phi(t+1)$  is introduced.

#### 4.1.2. Tent chaotic map

The GWO algorithm usually has poor optimization results in solving function optimization problems. The tent chaotic map [23] has better uniformity and can also improve the optimization speed of the algorithm. Therefore, this paper uses the tent chaotic map to initialize the population.

The tent chaotic map expression is as follows:

$$x_{t+1} = \begin{cases} \frac{x_t}{u}, & 0 \leq x_t \leq u \\ \frac{1-x_t}{1-u}, & u \leq x_t \leq 1 \end{cases}. \quad (18)$$

In this paper, we assumed that  $u = 1/2$ . Eq. (18) is changed to Eq. (19).

$$x_{t+1} = \begin{cases} 2x_t, & 0 \leq x_t \leq \frac{1}{2} \\ 2(1-x_t), & \frac{1}{2} \leq x_t \leq 1 \end{cases}. \quad (19)$$

#### 4.1.3. Dynamic weight

To improve GWO development capability and convergence speed, a nonlinear dynamic strategy weighting (NDSW) is added to the standard GWO algorithm. According to the algorithm, this will improve the global search performance of the GWO algorithm and the local development performance of the GWO algorithm.

The dynamic weights of the improved GWO (IGWO) algorithm [24,25] can be described as:

$$\omega = 0.5 + \frac{\text{rand}()}{2}. \quad (20)$$

In the GWO model, the maximum weight is 1, and the minimum weight is set to 0.001. rand() is the random number between 0 and 1.

In the improved algorithm, the formula of leader position change is as follows:

$$X_{\phi}(t+1) = \frac{\omega(X_{\alpha} + X_{\beta} + X_{\delta})}{3}. \quad (21)$$

In the process of the grey wolf position update, the first is to determine the impact of grey wolf individuals on the current t generation.

#### 4.2. Particle swarm optimization grey wolf algorithm to optimize back-propagation neural network

According to the prediction characteristics of the BP neural network, if the initial value of the system has a large deviation, the system prolongs the training time, reduces the prediction accuracy of the algorithm and causes the problem of local minima. To solve these important problems, this paper uses the PSO–GWO algorithm to optimize the weights and thresholds of the BP neural network in the initial state. (double written text). The steps of building the training model are shown in Fig. 2.

Since the units of the initial input variables are inconsistent, the raw data are normalized. Select 60 groups of “new energy photovoltaic power generation” data as training data and 30 groups as test data. Equation (22) is chosen as the fitness function

$$\text{Fitness} = \frac{1}{Z} \sum_{s=1}^Z (y_s - y'_s)^2, \quad (22)$$

where: Z is the training swatch number,  $y_s$  is the output value of network model,  $y'_s$  is the real output value. When the value of the fitness function reaches the minimum of the initial value, it is the optimal fitness value. We used optimized PSO–GWO initial weights and optimized thresholds as weights and thresholds of the BP network for data training. Then the PSO–GWO photovoltaic power generation prediction model was established.

Figure 3 is a graph of the parameter optimization process of PSO–GWO and GWO neural networks.

The number of iterations of the improved GWO algorithm is about 500. The optimization results gradually become stable. The optimal fitness value is  $8.325 \times 10^{-4}$ .

In programs, benchmarking is a method of testing code performance. For example, if you have different solutions to a problem, and you want to choose one with the best performance, this paper needs benchmarking. The test functions are shown in Table 1.

The optimal fitness images of PSO–GWO, GWO, MALO, SSA, DA and ALO optimized F1–F5 are shown in Fig. 4. The optimal fitness value refers to the maximum or minimum of the fitness function values obtained after multiple iterations in the six optimization algorithms, which

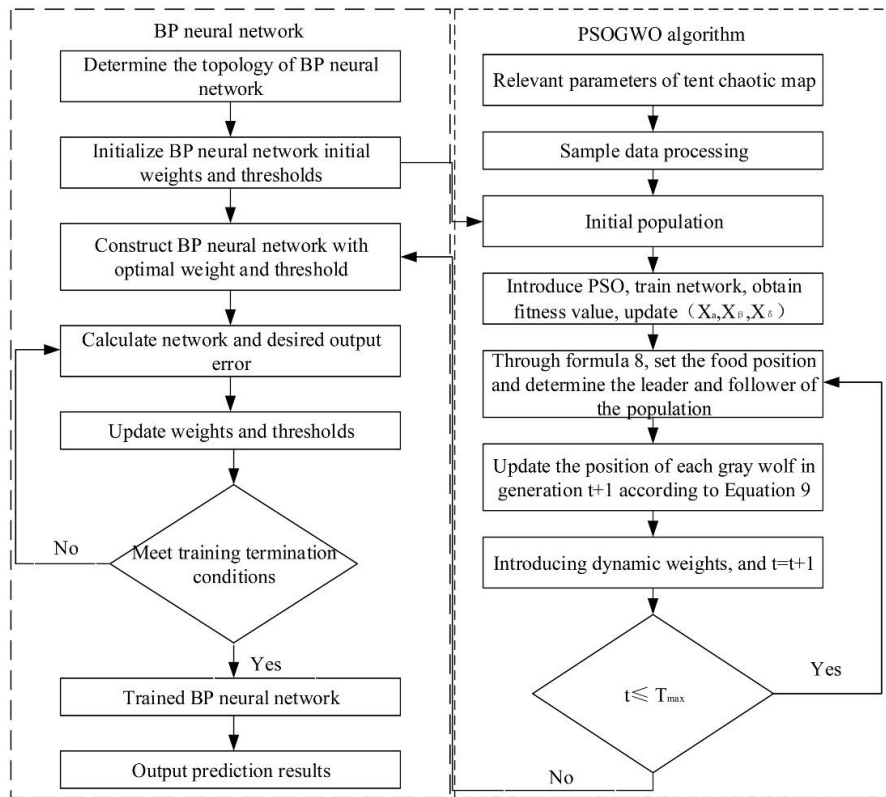


Fig. 2. Flowchart of PSO-GWO-BP neural network

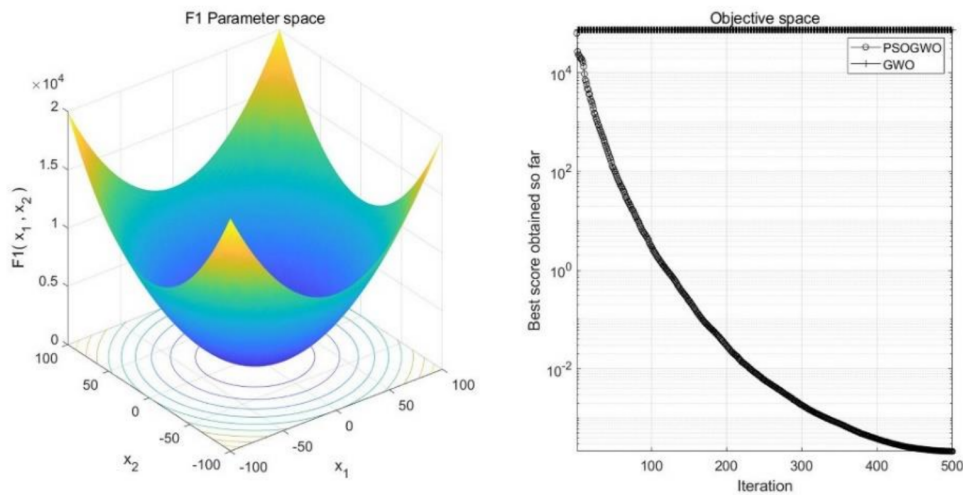


Fig. 3. Parameter optimization curve of PSO-GWO-BP and GWO-BP

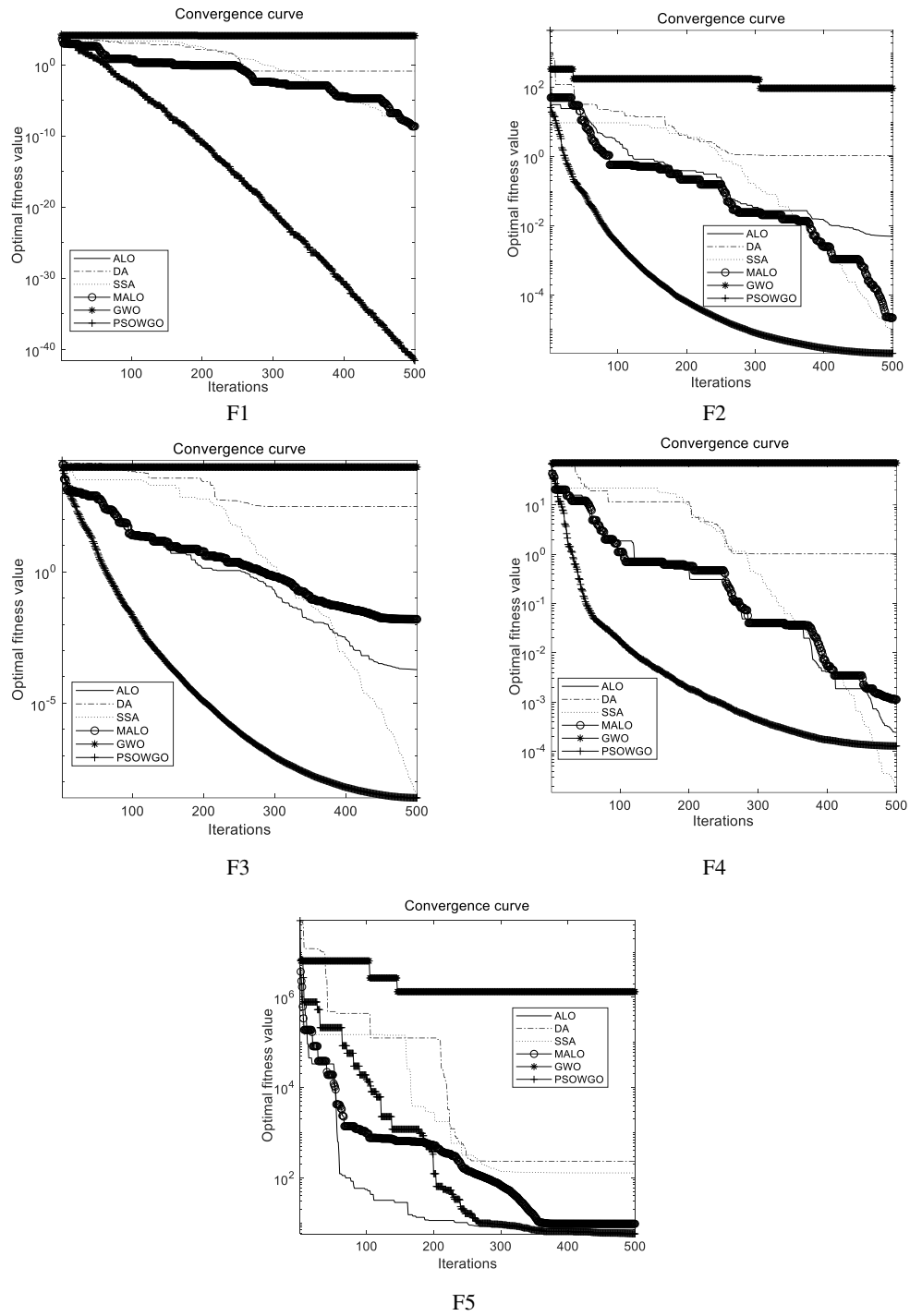


Fig. 4. Optimal fitness diagram of standard test function

Table 1. Benchmark function test results

| Function  | Dimension | Section     | Initial value |
|---|-----------|-------------|---------------|
| $F_1(x) = \sum_{i=1}^D x_i^2$   | 30        | [-100, 100] | 0             |
| $F_2(x) = \sum_{i=1}^D  x_i  + \prod_{i=1}^D  x_i $                             | 30        | [-10, 10]   | 0             |
| $F_3(x) = \sum_{i=1}^D \left( \sum_{j=1}^i x_j \right)^2$                       | 30        | [-100, 100] | 0             |
| $F_4(x) = \max_i \{ x_i , 1 < i \leq D\}$                                       | 30        | [-100, 100] | 0             |
| $F_5(x) = \sum_{i=1}^{D-1} \left[ 100(x_{i+1} - x_i^2)^2 + (x_i - 1)^2 \right]$ | 30        | [-30, 30]   | 0             |

represent the optimal solution or approximate value of the optimal solution that the algorithm can find. A higher optimal fitness value means that the algorithm can find a better solution, and vice versa, it means that the performance of the algorithm is poor. Therefore, the goal of the optimization algorithm is to find a better solution by continuously optimizing and improving the algorithm as close as possible to the optimal fitness value. The PSO–GWO in this paper allows for faster calculation speed and better performance, which can be obtained from Fig. 4 and Table 1.

## 5. Model trial calculation and analysis

### 5.1. Algorithm test

In this paper, to reflect the advantages of the proposed algorithm, the ant lion optimizer (ALO) algorithm, the dragonfly algorithm (DA), the salp swarm algorithm (SSA), the mutation ant lion optimization (MALO) algorithm, the grey wolf optimization (GWO) algorithm and the particle swarm optimization-grey wolf optimization (PSO–GWO) algorithm are selected. In order to make the algorithm fair, the conditions of these algorithms need to be set uniformly. The population is set to 40 and the number of iterations is set to 500. Through simulation testing, the simulation results are shown in Fig. 4 and Table 2. Figure 4 is the optimal fitness diagram of the standard test function. Table 2 shows the benchmark function test results.

This paper selects five benchmark functions to evaluate six models. In this paper, the performance of the improved grey wolf algorithm is verified by testing the ant lion optimizer (ALO) algorithm, the dragonfly algorithm (DA), the salp swarm algorithm (SSA), the mutation ant lion optimization (MALO) algorithm, the grey wolf optimization (GWO) algorithm and the

Table 2. Benchmark function test results

| Function |     | PSO–GWO          | GWO       | MALO      | SSA       | DA        | ALO       |
|----------|-----|------------------|-----------|-----------|-----------|-----------|-----------|
| $F_1$    | Ave | <b>2.745e-42</b> | 1.208e+04 | 2.299e-09 | 1.312e-09 | 0.1288    | 4.373e-09 |
|          | Std | <b>1.043e+06</b> | 6.881e+05 | 9.105e+04 | 1.011e+06 | 6.447e+05 | 3.684e+05 |
| $F_2$    | Ave | <b>4.765e-07</b> | 32.634    | 0.9903    | 7.045e-06 | 0.0845    | 4.654e-05 |
|          | Std | <b>2.804e+03</b> | 3.164e+03 | 36.172    | 12.113    | 5.328e+03 | 57.106    |
| $F_3$    | Ave | <b>3.539e-13</b> | 1.275e+04 | 0.0011    | 1.011e-08 | 1.186e+02 | 1.526e-05 |
|          | Std | <b>1.217e+06</b> | 3.254e+05 | 5.941e+05 | 3.252e+05 | 3.712e+07 | 5.006e+05 |
| $F_4$    | Ave | <b>3.196e-07</b> | 52.623    | 0.0013    | 9.758e-06 | 1.897     | 6.708e-04 |
|          | Std | <b>66.265</b>    | 51.998    | 31.166    | 62.906    | 2.631e+02 | 63.496    |
| $F_5$    | Ave | <b>5.531</b>     | 2.362e+07 | 3.432e+02 | 1.507e+02 | 1.534e+02 | 9.524     |
|          | Std | <b>5.021e+12</b> | 1.811e+14 | 8.789e+10 | 4.221e+09 | 1.151e+14 | 1.163e+12 |

particle swarm optimization-grey wolf optimization (PSO–GWO) algorithm. In order to compare the fairness, the average value and standard variance of  $F_1$ – $F_5$  are calculated. For the test function  $F_1$ – $F_5$ , the average value can reflect the optimization accuracy of the six algorithm models, the standard variance can directly reflect the robustness and stability of the six algorithm models.

According to the simulation experiment results, this can be seen from the  $F_1$ – $F_5$  test function. This paper proposes that the mean value and standard variance of PSO–GWO are significantly better than those of ALO, DA, SSA, MALO and GWO. In Fig. 4, PSO–GWO has fast optimization speed and high stability.

## 5.2. Model trial

In this paper, 90 groups of photovoltaic power generation sample data are used to establish the model. Among them, 60 groups of stochastic data are used as the training data of the neural network model for network training and the other 30 groups of sample data are used as the neural network test data. The prediction results of the photovoltaic power generation model were tested by these data. In order to compare the prediction results of different models, the input of input layer is used to build PSO–GWO–BP, GWO–BP and BP models.

## 5.3. Model error analysis

In order to fully understand the error of the three models, the relative error of the three models are compared. As shown in Fig. 5, the relative error of the PSO–GWO–BP model is smaller than that of the GWO–BP model and BP model. Among them, the relative error of the PSO–GWO–BP model is the smallest, the relative error of the BP model is the largest, and the relative error of the GWO–BP prediction model is slightly smaller than that of the BP prediction model.

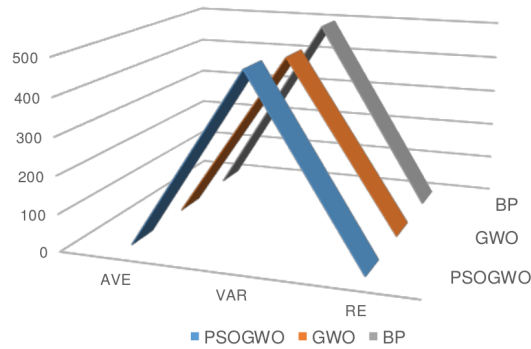


Fig. 5. Comparison of errors of prediction of three models

In order to further compare the prediction accuracy of the three models, the mean absolute error, mean absolute error variance and mean relative error of the three models are calculated. The prediction errors of each model are shown in Table 3.

Table 3. Comparison of forecast results evaluation

| Algorithm type | Average absolute error | Absolute error variance | Average value of relative error |
|----------------|------------------------|-------------------------|---------------------------------|
| <b>PSO–GWO</b> | 4.063                  | 422.77                  | 0.364                           |
| <b>GWO</b>     | 5.823                  | 459.65                  | 0.588                           |
| <b>BP</b>      | 6.394                  | 495.72                  | 0.416                           |

If the data set is small, the simple cross-validation method is generally adopted, that is, the verification set is not set, but only the training set and test set. According to many scholars, the ratio of the training set and test set is, generally, 2:1~ 4:1 [28]. According to the current learning method, most people set the ratio to 7:3.

If the data volume is large (some people say that the data set reaches 10 000), the distribution ratio of the training set, verification set and test set is 6:2:2 [29].

If the data volume is larger, for example, a million-level data set, the division ratio is generally more than 98:1:1 (that is, it increases the proportion of training set according to the situation) [28, 29]. Because this paper uses small amount of data, the ratio of the training set and test set is 7:3.

The three models are compared and analyzed as shown in Table 3. The GWO–BP model has the largest relative error, followed by the BP model. The relative error of the BP model is greater than that of the PSO–GWO–BP model, and the precision of the PSO–GWO–BP prediction model is the highest. The average absolute error of the PSO–GWO–BP model is the smallest and the average absolute error of the BP model is the largest. The variance of absolute errors of BP and GWO–BP is worse than that of PSO–GWO–BP. The average value of the absolute error and the variance of the absolute error show that the PSO–GWO–BP model has the strongest prediction stability and is more stable than the BP and GWO–BP prediction models. Based on the above

analysis we can say that the PSO–GWO–BP prediction model is the best and the BP prediction model is the worst.

## 6. Conclusion

So far, the BP neural network has a strong fitting ability. It is suitable for the application of complex internal mechanisms such as photovoltaic power systems. Because of the non-stationarity and randomness of the BP neural network, power generation is difficult to predict. In this paper, an improved grey wolf algorithm optimized BP neural network for photo-voltaic (PV) power prediction model is proposed. The dynamic weight strategy, tent mapping and particle swarm optimization (PSO) algorithm are introduced into the standard grey wolf optimization (GWO) algorithm to construct the PSO–GWO model. Predicting the output power of photovoltaic power stations can help the power system dispatching department to make overall arrangements for the coordination and cooperation of conventional energy and photovoltaic power generation, timely adjust the dispatching plan, and reasonably arrange the grid operation mode. On the one hand, it can effectively reduce the impact of photovoltaic access on the grid, improve the security and stability of grid operation, on the other hand, it can reduce the rotating reserve and operation costs of the power system, so as to make full use of solar energy resources, to achieve greater economic and social benefits.

The simulation results of the three models show that the relative error of the GWO–BP model is the largest, followed by BP. The relative error of the BP model is greater than that of the PSO–GWO–BP model, and the precision of the PSO–GWO–BP prediction model is the highest. The average absolute error of the PSO–GWO–BP model is the smallest and the average absolute error of the BP model is the largest. The variance of absolute errors of BP and GWO–BP is worse than that of PSO–GWO–BP. The average value of absolute error and the variance of absolute error show that the PSO–GWO–BP model has the strongest prediction stability and is more stable than the BP and GWO–BP prediction models. Through the above analysis, the PSO–GWO–BP prediction model is the best and the BP prediction model is the worst. In summary, in this paper, it is proposed that PSO–GWO–BP can improve the accuracy of photovoltaic power prediction, and this model has stronger applicability. In order to improve the stability of the power grid, the capacity of the power grid to absorb photoelectricity should be increased, which will help the photovoltaic power station reduce the economic losses caused by power limitation and improve the efficiency of the operation and management of the photovoltaic power station.

### Acknowledgments

The authors gratefully acknowledge the research funding provided by the National Natural Science Foundation of China (NSFC) (No. 52377125), the Scientific and Technological Research Foundation of Henan Province (No. 222102320198), and the Key Project of Zhengzhou University of Light Industry (2020ZDPY0204).

### References

- [1] Wang W.B., Zheng S.J., Chen W., *Performance evaluation index and method of microgrid distributed electric energy trading under the background of “carbon peaking and carbon neutrality”*, Journal of Shanghai Jiaotong University, vol. 55, no. 3, pp. 312–324 (2022), DOI: [10.16183/j.cnki.jsjtu.2021.391](https://doi.org/10.16183/j.cnki.jsjtu.2021.391).

- [2] Zhang K., Miao M., Zhang L.Q., *Carbon Peaking and Carbon Neutrality Goals and Reflections on China's Energy Transition Part I*, Sino-global Energy, vol. 27, no. 3 (2022).
- [3] Xin B.A., Shan B.G., Li Q.H., *Rethinking of the "Three Elements of Energy" Toward Carbon Peak and Carbon Neutrality*, Proceedings of the CSEE, vol. 42, no. 9, pp. 3117–3126 (2022), DOI: [10.13334/j.0258-8013.pcsee.212780](https://doi.org/10.13334/j.0258-8013.pcsee.212780).
- [4] Wei L.M., Li K.K., *Research on the output characteristics of photovoltaic arrays under partial shading conditions based on peak point approximate calculation method*, Archives of Electrical Engineering, vol. 71, no. 2, pp. 409–424 (2022), DOI: [10.24425/ae.2022.140719](https://doi.org/10.24425/ae.2022.140719).
- [5] Ke B., Ku T., Ke Y., *Sizing the Battery Energy Storage System on a University Campus with Prediction of Load and Photovoltaic Generation*, IEEE Transactions on Industry Applications, vol. 52, no. 2, pp. 1136–1147 (2016), DOI: [10.1109/TIA.2015.2483583](https://doi.org/10.1109/TIA.2015.2483583).
- [6] Zhang J.P., Wang B.N., Huang R., *Survey on frequency regulation technology of power grid by high-penetration photovoltaic*, Power System Protection and Control, vol. 47, no. 15, pp. 179–186 (2019), DOI: [10.19783/j.cnki.pspc.181042](https://doi.org/10.19783/j.cnki.pspc.181042).
- [7] Zhang F., Zhang F., *Power Load Forecasting in the Time Series Analysis Method Based on Lifting Wavelet*, Power System Automation, vol. 39, no. 3, pp. 72–76 (2017), DOI: [10.7500/AEPS20180603002](https://doi.org/10.7500/AEPS20180603002).
- [8] Li M.K., Wang Y., Sun G., *Research on fault location method of UHVDC grounding pole line based on regression analysis*, Electrical Measurement Instrumentation, vol. 58, no. 9, pp. 129–134 (2021), DOI: [10.19753/j.issn1001-1390.2021.09.019](https://doi.org/10.19753/j.issn1001-1390.2021.09.019).
- [9] Abedinia O., Amjady N., Ghadimi N., *Solar energy forecasting based on hybrid neural network and improved metaheuristic algorithm*, Computational Intelligence, vol. 34, no. 1, pp. 241–260 (2018), DOI: [org/10.1111/coin.12145](https://doi.org/10.1111/coin.12145).
- [10] Zhu H., Wang Y., *Intelligent Prediction of Prestressed Steel Structure Construction Safety Based on BP Neural Network*, Applied Sciences, vol. 12, no. 1, pp. 1442 (2022), DOI: [10.3390/app12031442](https://doi.org/10.3390/app12031442).
- [11] Al-Dahidi S., Ayadi O., Alrbai M., Adeeb J., *Ensemble Approach of Optimized Artificial Neural Networks for Solar Photovoltaic Power Prediction*, IEEE Access, vol. 7, pp. 81741–81758 (2019), DOI: [10.1109/ACCESS.2019.2923905](https://doi.org/10.1109/ACCESS.2019.2923905).
- [12] Yuan X.L., Shi J.H., Xu J.Y., *Short-term power forecast for photovoltaic generation based on BP neural network*, Renewable Energy Resources, vol. 31, no. 7, pp. 11–16 (2013), DOI: [10.13941/j.cnki.21-1469/tk.2013.07.019](https://doi.org/10.13941/j.cnki.21-1469/tk.2013.07.019).
- [13] Ding M., Wang L., Bi R., *A short-term prediction model to forecast output power of photovoltaic system based on improved BP neural network*, Power System Protection and Control, vol. 40, no. 11, pp. 93–99+148 (2012), DOI: [10.13941/j.cnki.21-1469/tk.2013.07.019](https://doi.org/10.13941/j.cnki.21-1469/tk.2013.07.019).
- [14] Chui X., Fang J.L., Qu L., *Photovoltaic power prediction based on PSO-BP algorithm*, Heilongjiang Electric Power, vol. 43, no. 2, pp. 109–112+117 (2021), DOI: [10.13625/j.cnki.hljep.2021.02.004](https://doi.org/10.13625/j.cnki.hljep.2021.02.004).
- [15] Tang X., Dai Y., Wang T., *Short-term power load forecasting based on multi-layer bidirectional recurrent neural network*, IET Generation, Transmission & Distribution, vol. 13, no. 17, pp. 3847–3854 (2019), DOI: [10.1049/iet-gtd.2018.6687](https://doi.org/10.1049/iet-gtd.2018.6687).
- [16] Li Y.C., Ma L.Q., *Fault diagnosis of power transformer based on improved particle swarm optimization OS-ELM*, Archives of Electrical Engineering, vol. 68, no. 1, pp. 161–172 (2019), DOI: [10.24425/ae.2019.125987](https://doi.org/10.24425/ae.2019.125987).
- [17] Ahmed A. Shehata, Ahmed Refaat, Mamdouh K. Ahmed, Nikolay V. Korovkin, *Optimal placement and sizing of FACTS devices based on Autonomous Groups Particle Swarm Optimization technique*, Archives of Electrical Engineering, vol. 70, no. 1, pp. 161–172(2021), DOI: [10.24425/ae.2021.136059](https://doi.org/10.24425/ae.2021.136059).

- [18] Cao Y., Gao B.P., Zhang Z.H., *A fault diagnosis method for power grid based on PSO–GWO*, *Electrical Measurement and Instrumentation*, vol. 58, no. 9, pp. 35–40 (2021), DOI: [10.19753/j.issn1001-1390.2021.09.006](https://doi.org/10.19753/j.issn1001-1390.2021.09.006).
- [19] Dhal Pradip, Azad Chandrashekhar, *A multi-objective feature selection method using Newton's law based PSO with GWO*, *Applied Soft Computing Journal*, vol. 107, pp. 107394 (2021), DOI: [10.1016/j.asoc.2021.107394](https://doi.org/10.1016/j.asoc.2021.107394).
- [20] Gao X., Liu C.L., Cao M., *Load forecasting based on VMD and Support Vector Machine Optimized by Hybrid PSO–GWO*, *Mathematics in Practice and Theory*, vol. 51, no. 19, pp. 235–242 (2021).
- [21] He S.M., Yuan Z.Y., *Optimal setting method of inverse time over-current protection for a distribution network based on the improved grey wolf optimization*, *Power System Protection and Control*, vol. 49, no. 18, pp. 173–181 (2021), DOI: [10.19783/j.cnki.pspc.201351](https://doi.org/10.19783/j.cnki.pspc.201351).
- [22] Wu Y.X., Gao C., Cao H.Z., *Clustering analysis of daily load curves based on GWO algorithm*, *Power System Protection and Control*, vol. 48, no. 6, pp. 68–76 (2020), DOI: [10.19783/j.cnki.pspc.190486](https://doi.org/10.19783/j.cnki.pspc.190486).
- [23] Tian S.X., Liu L., Wei S.R., *Dynamic reconfiguration of a distribution network based on an improved grey wolf optimization algorithm*, *Power System Protection and Control*, vol. 49, no. 16, pp. 1–111 (2021), DOI: [10.19783/j.cnki.pspc.201356](https://doi.org/10.19783/j.cnki.pspc.201356).
- [24] Zhang W.T., Zhang D.P., *Soft Sensor Model of SCR Denitration Efficiency Based on IGWO–BP*, *Computer Measurement and Control*, vol. 29, no. 10, pp. 66–70+76 (2021), DOI: [10.16526/j.cnki.11-4762/tp.2021.10.012](https://doi.org/10.16526/j.cnki.11-4762/tp.2021.10.012).
- [25] Li X.W., Chen C., Tao Y.G., *Comprehensive evaluation of distribution network connection mode based on IGWO–BP*, *Electronic Measurement Technology*, vol. 43, no. 3, pp. 71–76 (2020), DOI: [10.19651/j.cnki.emt.1903358](https://doi.org/10.19651/j.cnki.emt.1903358).
- [26] Liang E.H., Sun J.W., Wang Y.F., *Wind and solar complementary grid-connected power generation prediction based on BP optimized by a swarm intelligence algorithm*, *Power System Protection and Control*, vol. 49, no. 24, pp. 114–120 (2021), DOI: [10.19783/j.cnki.pspc.210059](https://doi.org/10.19783/j.cnki.pspc.210059).
- [27] Teng Y.J., Lv J.L., Guo L.W., *An improved hybrid grey wolf optimization algorithm based on Tent mapping*, *Journal of Harbin Institute of Technology*, vol. 50, no. 11, pp. 40–49 (2018), DOI: [10.11918/j.issn0367-6234201806096](https://doi.org/10.11918/j.issn0367-6234201806096).
- [28] Hu Y., Wei Y., Zhang H., *Using machine learning to predict two-phase flow regimes in horizontal pipes*, *International Journal of Heat and Mass Transfer*, vol. 120, pp. 1043–1053 (2018), DOI: [10.1016/j.ijheatmasstransfer.2017.12.110](https://doi.org/10.1016/j.ijheatmasstransfer.2017.12.110).
- [29] Kailkhura B., Chakraborty T., *A systematic study of the effect of feature normalization on the performance of machine learning models in classifying medical images*, *Journal of Medical Systems*, vol. 43, no. 6, pp. 137 (2019), DOI: [10.1007/s10916-019-1297-8](https://doi.org/10.1007/s10916-019-1297-8).